

# Preliminary assessment of the scaling relationships of in-situ stress orientation variations indicated by wellbore failure data

B. Valley & K. F. Evans

*Geological Institute, ETH Zürich, Switzerland*

**ABSTRACT:** Borehole failure data provides a unique insight in the characteristics of the stress field because in deep boreholes it tends to be pervasive, providing the opportunity to study variability of the stress components. This variability might follow self-affine scaling and could be related to scaling characteristics of the natural fractures network and earthquake magnitude-frequency statistic. If this were the case, then the measurable variations in stress orientation could be used to constrain statistical attributes of the fracture network and to anticipate the seismic response of a rock mass. In this paper, we evaluate seven techniques to determine the fractal dimension,  $D$ , of stress orientation variations indicated by wellbore failure data by applying them first to synthetic data of known fractal dimension. Particular attention was given to assess the biases introduced by the presence of gaps and noise in the data. Finally, the evaluation techniques were applied to real borehole failure data from Soultz-sous-Forêts and Basel. Preliminary results indicate that significantly different estimates of  $D$  were found for different methods applied to the same dataset which are best explained as reflecting the impact of gaps in the data.

## 1 INTRODUCTION

Knowledge of stress distribution is central to rock mass characterization of deep engineering projects. Wellbore failure provides an opportunistic window for defining stress state because at large depth it tends to be pervasive. In such cases it is possible to generate almost continuous profiles of certain attributes of the stress tensor and hence evaluate the nature of the variability that is seen.

There are indications that in-situ stress variations, as many other geological phenomena, might follow self-affine scaling (Turcotte and Huang, 1995). It is hypothesized that such scaling characteristics are intimately related to the scaling characteristics of the fracture network and earthquake magnitude-frequency statistics (Day-Lewis et al., 2010). If this were the case, then the measurable variations in stress orientation could be used to constrain statistical attributes of the fracture network that are difficult to estimate, and to anticipate the seismic response of a rock mass to hydraulic injections.

In order to be of practical value, the scaling characteristics of stress variability must be reliably determined. This paper evaluates various methods for estimating the scaling characteristics of stress variations by applying them on synthetic series of known fractal dimension. We also evaluate the ability of the methods to deal with gaps in the record and measurement inaccuracy, which is common for borehole failure data. Finally, the various methods are applied to real data sets from three 5 km deep boreholes at Soultz-sous-Forêts and Basel to compare the estimates of fractal dimension of the stress series.

## 2 FRACTAL DIMENSION OF 1-D SIGNALS

Fractal mathematical models are useful to describe geometries that have no characteristic size or length

scale. Statistical fractals are objects that are not exactly identical when changing scale but that conserve their statistical attributes. In this paper we will deal with a one-dimensional series  $V(x)$  (e.g. a quantity that varies with time or distance). Fractal distributions are parameterized by the fractal dimension  $D$  that captures how details in a pattern change with the observation scale. It is also a measure of the space-filling capacity. That is, the fractal dimension of a one-dimensional function may vary from  $D = 1$ , for which the graph is a straight line, to  $D = 2$ , which is a very variable quantity whose graph will be a very rough line. The distinction between self-similarity and self-affinity is related to the conservation of statistical properties upon magnification of a profile (e.g. Brown, 1995). Self-similar shapes repeat themselves (exactly or statistically) under a magnification with equal scaling for both axis  $x$  and  $V(x)$  axis. Self-affine shapes, however, need different (but constant) scaling factors to conserve their properties.

## 3 GENERATION OF SYNTHETIC FRACTAL DATA

We use fractional Brownian motion (fBm) of known fractal dimension in order to test approaches to determine the fractal dimension. The Hurst exponent,  $H$ , controls the scaling behavior of fractional Brownian motion by the simple scaling law  $\Delta V \propto \Delta x^H$ . The Hurst exponent takes value in the range  $0 < H < 1$ . For one dimensional signal, it is related to the fractal dimension by:

$$D = 2 - H \quad (1)$$

Pure Brownian motion series can be generated by integrating white noise, (i.e. successive random draws from a normal distribution). Such a series will have a fractal dimension  $D = 1.5$ . Fractional Brownian motion with other fractal dimensions can

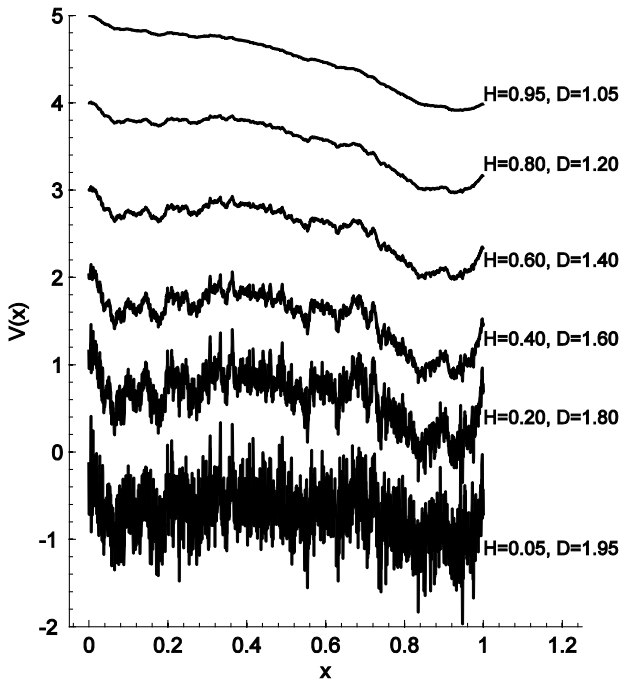


Figure 1: Synthetic discrete fractional Brownian motion signal with known fractal dimension. Here signal are scaled and offset for proper visibility. Each series contains 2048 data points.

be generated using various algorithms summarized by Saupe (1988).

The series we used were generated using a frequency domain method developed by Davies and Harte (1987) with a modification from Percival (1992) and Wood and Chan (1994). This algorithm has been implemented in FORTRAN by the Physiome project at the National Simulation Resource Center for Bioengineering at the University of Washington (Physiome Project, 2013). It is superior to midpoint displacement methods since it generates a series with both the correct fractal dimension and autocorrelation function (Percival, 1992). Examples of series generated with this algorithm with fractal dimension varying from 1.05 to 1.95 are shown in Fig. 1.

## 4 METHODS FOR ESTIMATING FRACTAL DIMENSION

Three types of method were tested: divider and box counting methods, windowed variance methods and power spectrum methods. These methods are introduced in the following sections.

### 4.1 Divider and box counting methods

Divider and box counting methods are perhaps closest to the original definition of the fractal dimension. Brown (1995) presents improved divider and counting box methods to determine the fractal dimension of self-affine fractals. The divider method is performed conceptually by opening a pair of dividers to some distance  $r$  and walking them along the curve of the series to measure its total length  $\lambda$  (Brown, 1995). The slope of the total measured length  $\lambda$  vs.  $r$

in a log-log plot gives an estimate of the fractal dimension using the following relation:

$$\lambda \propto r^{1-D} \quad (2)$$

As noted by Brown (1995), the method breaks down if the divider length  $r$  is not much smaller than the series amplitude variations. This can be remedied by iteratively multiplying the series, an operation which does not affect the fractal dimension, until  $r$  is small compared to the series variations and a stable determination of  $D$  with increasing magnification is achieved.

For the box counting method, the fractal dimension is estimated by laying a grid with  $n^2$  cells over the curve and counting the number of cells  $N(n)$  covering the signal. For self-affine series, the aspect ratio of the cells used can introduce bias in the determination of  $D$ . To prevent such bias, Brown (1995) suggests using an aspect ratio for the cells of  $\lambda_0/6\sigma_0$ , where  $\lambda_0$  is the nominal length of the signal, i.e. its length along the  $x$ -axis,  $\sigma_0$  is its standard deviation. With this approach, the fractal dimension is estimated by determining the slope of the relation  $N(n)$  vs.  $n$  on a log-log plot with the following formula:

$$N(n) \propto n^D \quad (3)$$

### 4.2 Windowed variance methods

Cannon et al. (1997) introduced the scaled windowed variance (SWV) methods for estimating the Hurst exponent  $H$  of fractional Brownian motion series. The principle is to repeatedly divide the series into sets of windows of length  $s$ -points, and compute the mean of the standard deviations of each set of windows  $\overline{SD}(s)$  as a function of  $s$ . The Hurst exponent is estimated on a log-log plot of  $\overline{SD}(s)$  vs.  $s$  by the following relation:

$$\overline{SD}(s) \propto s^H \quad (4)$$

Implementation of the method without detrending the series in each window will be referred to here as the standard SWV approach. Cannon et al. (1997) also proposed two variations where the series in each window was detrended before computing the standard deviation in order to reduce bias and variability in the estimate of  $H$ . Detrending is achieved by subtracting a linear regression line for each interval (denoted here as LD-SWV) or a bridge (i.e. straight line from first and last point) over the interval (BD-SWV). Details of the implementation are given in Cannon et al. (1997). The algorithms were implemented in FORTRAN by the Physiome Project (2013).

### 4.3 Power density spectrum methods

The power spectral density (PSD),  $S_v(f)$ , where  $f$  is the frequency, for a series  $V(x)$  is an estimate of the

mean square fluctuation of the series at frequency  $f$ . For a fractal series, the PSD spectrum has a slope of  $1/f^\beta$ , and thus declines linearly with frequency with a slope of  $-\beta$  in a  $\log Sv(f)$  vs.  $\log f$  plot. The slope  $\beta$  is referred as the spectral index. For a one-dimensional fractal signal,  $\beta$  lies in the range  $1 < \beta < 3$ , and is related to the fractal dimension by:

$$D = \frac{5 - \beta}{2} \quad (5)$$

The options to determine  $D$  using PSD methods are thus distinguished by the approach used to determine the power density spectrum. We used two approaches: 1) a fast Fourier transform with pre-filtering of the data using a Hanning window (FFT) and 2) an algorithm proposed by Broerson et al. (2004) that can deal with gap in the data (BROERSON). Both methods are implemented in MATLAB<sup>TM</sup>. The fast Fourier transform and Hanning window function are part of commercial MATLAB<sup>TM</sup> distributions. The algorithm by Broerson et al. (2004) is provided by the authors through the MATLAB<sup>TM</sup> Central File Exchange ([www.mathworks.com](http://www.mathworks.com)).

## 5 EVALUATION ON SYNTHETIC DATA

The methods of estimating the fractal dimension,  $D$ , are evaluated and compared by applying them to synthetic series of known fractal dimension. It is assumed that the true fractal dimensions of the generated series corresponds to the expected values. Although we cannot be sure of this, some small deviation can be tolerated since the primary objective is to compare the  $D$ -estimates from the different methods rather than the absolute value of  $D$ . The processing is applied first on clean synthetic data and then on series degraded by adding noise or gaps.

### 5.1 Clean continuous data

A comparison of the  $D$ -estimates obtained by applying each method to clean data series of known fractal dimension in the range  $D = 1.0$  to  $2.0$  is presented on Fig. 2. Each estimate was made over 100 randomly generated fractal series with 2048 data points (similar to the series shown in Fig. 1). The median, lower- and upper-quartile values of  $D$  obtained for the 100 realizations is displayed as a function of the expected fractal dimension of the generated series. A perfect estimation of  $D$  would plot on the 1:1 lines that are drawn for convenience (note that the curves have been offset to facilitate readability).

Fig. 2 suggests that the windowed variance methods generally yield the best estimations of  $D$  over the range considered. The estimates of  $D$  are slightly high, particularly for low  $D$ , but the medians are always within 0.04 and the quartiles within 0.08 of the expected value for the series. The next best estimates

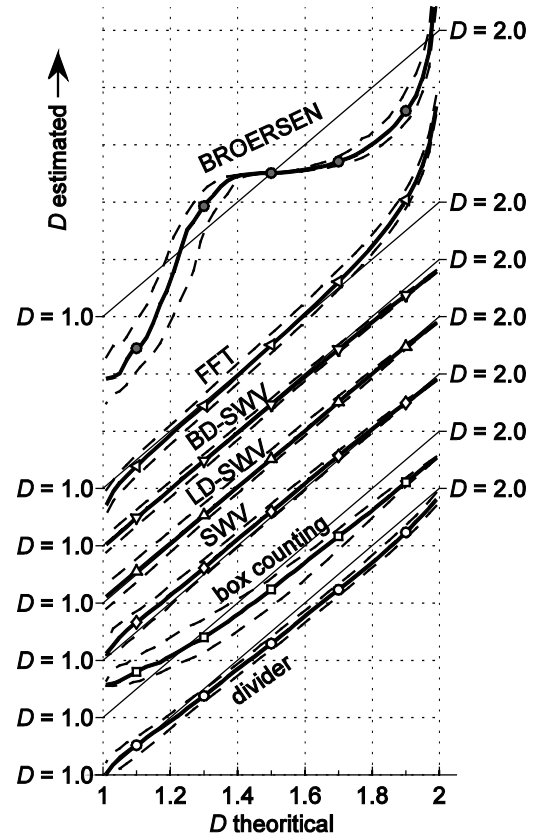


Figure 2: Evaluation of the accuracy of methods for estimating  $D$  of synthetically-generated series whose  $D$ -value is known and ranges between 1.0 and 2.0. The series have 2048 data points. The solid and bounding dashed lines denote median and lower and upper quartiles of estimate distributions computed over 100 randomly generated series.

are obtained from the divider method. This tends to underestimate the value of  $D$ , particularly for high  $D$ , but the medians are always within 0.06 of the expected value. The variation in the  $D$ -estimates over the 100 realizations for the SWV and divider methods is small, as shown by the narrow interquartile range that widens for lower  $D$  but is always less than 0.09.

The box counting method tends to overestimate  $D$  for theoretical  $D < 1.25$  and to underestimate for  $D > 1.25$ . The quartiles of the estimates are always within 0.14 or better of the expected value of  $D$ . The interquartile range is 0.12 or smaller, indicating somewhat less consistent estimate of  $D$  than for the four methods discussed above.

The FFT method with the Hanning window gives a good estimate of  $D$  with very little bias and an interquartile range of about 0.08 for theoretical  $D$  below 1.7. Above 1.7, the value of  $D$  is overestimated. It is important to apply a window function that smoothly sets the data to zero at the start and end of the series, such as the Hanning, in order to get reasonable results.

The impact of series length on the accuracy of the fractal dimension estimates was evaluated for series with expected fractal dimension  $D = 1.2, 1.5$  and  $1.8$  by varying series length from 128 to 8192 data points. Generally, the interquartile range of the esti-

mates increased with decreasing series length. For example, for the DIVIDER method, the interquartile range of the estimate of  $D$  for expected  $D = 1.5$  increases from 0.03 for a series length of 8192 points to 0.11 for a series length of 128 points. For the DIVIDER, SWV and LD-SWV, the median of the estimates is not much affected by decreasing series length, whereas for other methods it increases the discrepancy between the estimated median and expected value of  $D$ . For example, for the box counting method, the median of the estimate of  $D$  for a series with expected  $D = 1.8$  increases from 0.05 for a series length of 8192 data points to 0.16 for a series length of 128 data points. For all methods, lengthening the series beyond 1024 data points does not significantly improve the median of the estimates of  $D$ , except for the BOX and BROERSON methods for whose improvements persists up to 8192 data points.

### 5.2 Data with noise

Noise is invariably present in a series describing the measured variation of any physical variable. For the case of interest, that of profiles of the orientation of the maximum horizontal stress, SHmax, from say borehole breakouts, the uncertainty in determining the center point of the breakout will add some noise to the SHmax-orientation estimates. The impact of such random noise on the estimates of fractal dimension of the synthetic fractal series is evaluated by adding Gaussian noise to the data. The results shown Fig. 3, correspond to the case where the standard deviation of the added Gaussian noise is 1/60 of the total range covered by the series. This scaling is necessary because the range of series of different fractal dimension generated by the algorithm varied over several orders of magnitude. Normalizing by a fraction of the range thus simulates the case of adding constant amplitude noise to series of the same range (such as those shown in Fig. 1). Series of 2048 data-points length were used. For all methods, the impact of the noise is to give progressively greater overestimates of  $D$  for series whose theoretical  $D$  less than 1.5, except for the BROERSON method because the estimate of  $D$  is already strongly underestimated without the presence of noise (see Fig. 2). The method that is most resistant to the added noise is the box counting method. The maximum discrepancy between estimated and expected  $D$  occurs for  $D = 1$  and is about 0.34. For the divider and windowed variance methods, this difference reaches 0.9.

Generally, random noise added to the data will have a severe impact on the determination of the fractal dimension when  $D < 1.5$ . If the underlying signal has a fractal dimension smaller than 1.5, it is very likely that the determined fractal dimension will be overestimated.

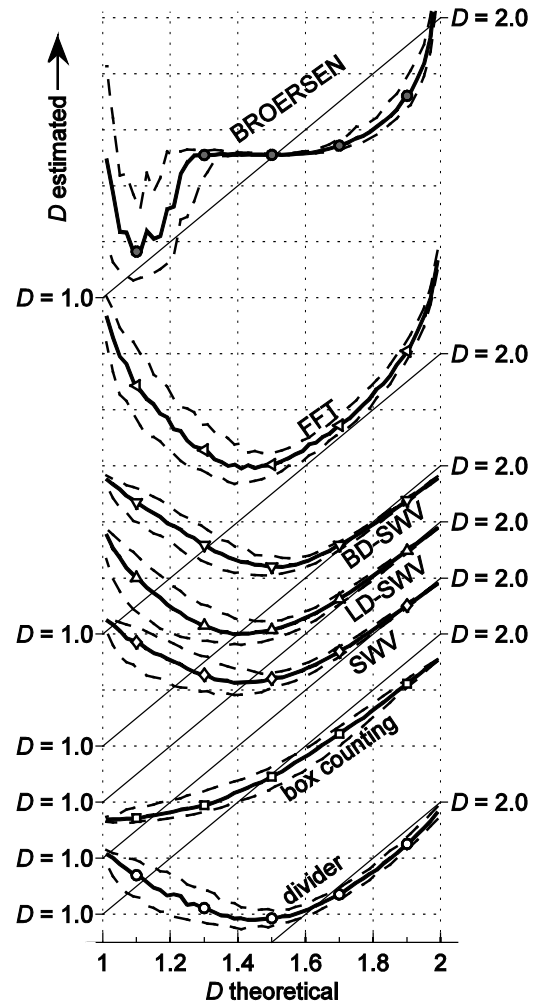


Figure 3: Evaluation of the accuracy of methods for estimating  $D$  when random noise is added to the fractal series. Gaussian noise with a standard deviation of 1/60 of the range of the fractal series is added. The series length is 2048 data points.

### 5.3 Data with gaps

Typically, wellbore failure is not continuous, and thus the series describing the variation of a stress attribute along the borehole will include gaps. The effect of gaps in the data on the estimates of  $D$  is evaluated by randomly adding gaps to the synthetic fractal series. Two parameters were used to control the application of gaps to the data: 1) the percentage of missing data, which can vary between 0% for continuous data to 100% for no data, and 2) the number of gaps. For the same percentage of missing data, if the number of gaps is higher, the gaps will generally be shorter. However, the actual size and location of the gaps is random.

In all but the BROERSON method, the gaps were filled by straight lines (i.e. linear interpolation) prior analysis. In the BROERSEN case, a special version of the algorithm specifically designed for the missing data problem was used to derive the power spectra (Broersen et al., 2004).

Fig. 4 shows a comparison of the  $D$ -estimates for the case where 35% of the data are missing, distributed over 40 gaps. The estimates for the FFT method with Hanning window are not much affected by the

presence of gaps. For the BROERSON method, the primary effect of the gaps is to produce larger deviations from the expected  $D$ -estimates for  $D < 1.5$ . In all other cases, the primary effect of the gaps is to result in systematic underestimation (i.e. negative bias) of  $D$  at all but the lowest  $D$ -values. For the box counting, standard SWV, and LD-SWV methods, the underestimate is about 0.1, and for the divider and BD-SWV methods it is slightly larger. The bias generally becomes more pronounced when the percentage of missing data increases. For example, in the case of the SWV method, the bias increases to about 0.25 when 80% of the data are missing. The FFT method is the most resistant to bias, with an underestimation of  $D$  less than 0.12 even for 80% of missing data. The number of gaps also has an influence on the determination of  $D$ . The bias is most pronounced when 20 to 30 gaps are present, and is less when the number of gaps is lower or larger.

## 6 APPLICATION ON REAL STRESS DATA

In this section, the various methods of determining fractal dimension are applied to real borehole failure data. The data sets stem from three deep boreholes: GPK3 and GPK4 located at the Soultz- sous-Forêts EGS site in France, and borehole BS1 at Basel in Switzerland. The original data for Soultz-sous-Forêts are presented in Valley and Evans (2010) and for Basel in Valley and Evans (2009). The data sets consist of profiles of SHmax-orientation derived from wellbore failure indicators.

In the case of Soultz-sous-Forêts, the orientation of the features were determined over successive 0.5 m windows. At Basel, the orientation of the features were determined every 0.4 m. For each well, the mean SHmax-orientation was subtracted from the data in order to keep only the variation from the mean. The data were prepared for the analyses by resampling at a uniform spacing of 0.1 m. Only subsections of the datasets where the SHmax-orientation estimates are relatively continuous are considered for the analyses performed in this paper.

The prepared data sets are presented in Fig. 5, and a summary of their key characteristics is given in Table 1. For GPK3 and GPK4, the SHmax-estimates in the selected intervals are derived largely from drilling induced tension fractures. For BS1 the estimates stem principally from borehole breakouts.

The fractal dimension estimates obtained by applying the seven methods to each of the three data sets are summarized in Fig. 6. The interpretation of the results is not trivial since large variability between the estimates for a given borehole is evident. The methods that yielded the most reliable results across the entire range of  $D$ -values in the study with synthetic data were the DIVIDER, SWV, LD-SWV BD-SWV methods, whilst the FFT method yielded

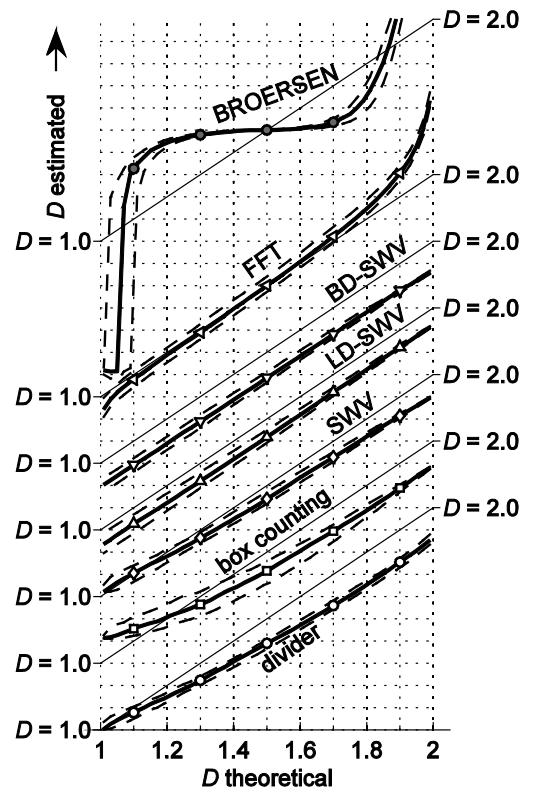


Figure 4: Evaluation of the impact of gap on the estimates of  $D$ . In this example, 35% of the data were removed distributed over 40 gaps.

the best results in the presence of gaps for expected  $D$ -values less than 1.8. The low values obtained from the DIVIDER and BD-SWV methods probably reflect the effect of the gaps. The study on synthetic data indicated these methods more strongly underestimate  $D$  in the presence of gaps, and the discrepancy with the other methods is not so marked for the BS-1 data, which contains far fewer gaps. The studies with synthetic data with gaps also suggest the estimates of  $D$  from the BOX, BROERSON and SWV methods would be somewhat low since  $D$  is clearly greater than 1.5, and that the best estimate of  $D$  would come from the FFT method. If this is accepted, then the best estimate of  $D$  for both GPK4 and BS1 is 1.77, whilst for GPK3 it is 1.66. It is also evident that the BOX and SWV estimates of  $D$  for GPK4 and BS1 are comparable, whilst those for GPK3 are lower, although only marginally so. The important conclusion is that there is more similarity in the range of  $D$ -estimates between GPK4 and BS1 than there is between GPK3 and 4, despite the fact that they sample essentially the same rock volume.

Table 1: Summary of key characteristics of the prepared data

Hole	GPK3	GPK4	BS1
Interval	1495 – 2195 m	1511 – 2186 m	2618 – 5000 m
Length	700 m	675 m	2382 m
Number of data point	7001	6751	23820
% of missing data	36%	35%	19%
Number of gaps	41	43	115
Longest continuous data section	63 m	44 m	99 m
Longest gap	24 m	35 m	80 m

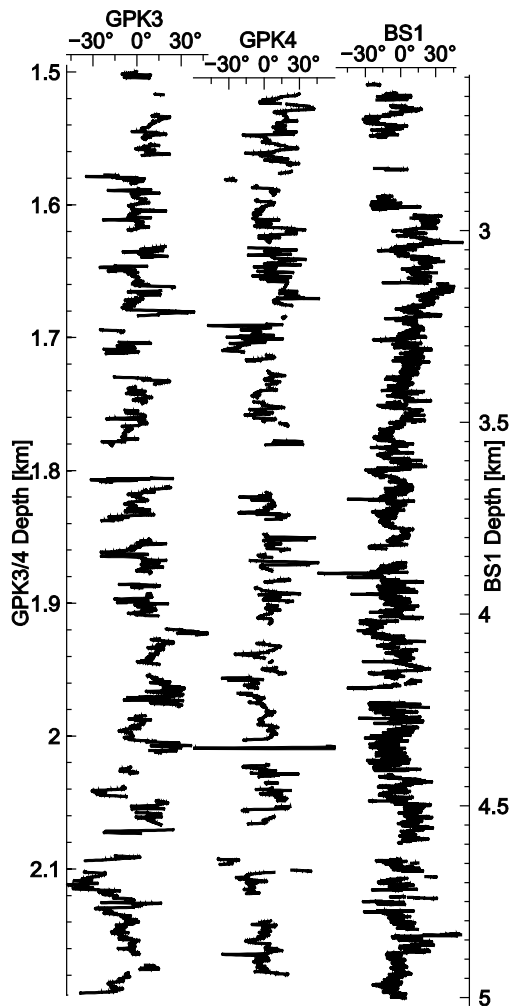


Figure 5: Sections of the GPK3, GPK4 and BS1 data sets used in this paper.

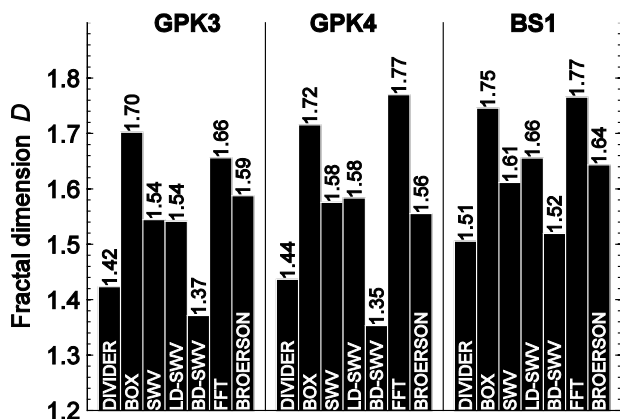


Figure 6: Fractal dimension estimate for the three data sets investigated using the eight methods presented above.

## 7 CONCLUSION

The determination of fractal dimension from borehole failure data is not a trivial exercise. Biases can occur because the data contain noise and gaps.

The assessment performed in this paper used synthetic series of known fractal dimension to test the various methods for estimating  $D$ . The effect of gaps and noise in the data on the estimates was evaluated. The FFT method was found to yield the best estimates of  $D$  when gaps were present, as is often the

case with stress profiles from wellbore failure data. The various methods were then applied to real data sets from Soultz-sous-Forêts and Basel. Significantly different estimates of  $D$  were found for different methods applied to the same dataset which are best explained as reflecting the impact of gaps in the data.

## 8 ACKNOWLEDGMENTS

This work is funded by the GEOTHERM-2 research program supported by the Competence Center for Environment and Sustainability (CCES) and the Competence Center Energy and Mobility (CCEM) of ETH Domain, and the Swiss Federal Office of Energy.

## REFERENCES

- Broersen, P. M. T., de Waele, S. & Bos, R. 2004. Application of autoregressive spectral analysis to missing data problems. *IEEE Transactions on Instrumentation and Measurement* 53 (4), 981–986.
- Brown, S. R., 1995. Measuring the dimension of Self-Affine Fractals: example of rough surfaces. In: *Fractal in the earth sciences*, Barton & La Pointe (eds). Plenum Press, New York.
- Cannon, M. J., Percival, D. B., Caccia, D. C., Raymond, G. M. & Bassingthwaite, J. B. 1997. Evaluating scaled windowed variance methods for estimating the hurst coefficient of time series. *Physica A: Statistical Mechanics and its Applications* 241 (3-4), 606–626.
- Davies, R. B. & Harte, D. S. 1987. Tests for Hurst effect. *Biometrika* 74 (1), 95–101.
- Day-Lewis, A., Zoback, M. & Hickman, S. 2010. Scale-invariant stress orientations and seismicity rates near the San Andreas fault. *Geophysical Research Letters* 37 (24), L24304+.
- Percival, D. B., 1992. Simulating gaussian random processes with specified spectra. In: Page, C., LePage, R. (Eds.), *Computing Science and Statistics, Proceedings of the 22nd Symposium on the Interface*. Springer, pp. 534–538.
- Physiom Project, 2013. Fractal analysis programs of the national simulation resource. <http://bioeng.washington.edu/software/fractal/>, accessed: 2013-11-15.
- Raymond, G. M., Percival, D. B. & Bassingthwaite, J. B., 2003. The spectra and periodograms of anti-correlated discrete fractional gaussian noise. *Physica A* 322, 169–179.
- Saupe, D., 1988. Algorithms for random fractals. In: *The science of fractal images*, Peitgen & Saupe (eds) Springer Verlag.
- Turcotte, D. L. & Huang, J., 1995. Fractal distribution in geology, scale invariance, and deterministic chaos. In: *Fractal in the earth sciences*, Barton & La Pointe (eds). Plenum Press, New York.
- Valley, B., Evans, K. F., 2010. Stress heterogeneity in the granite of the Soultz EGS reservoir inferred from analysis of wellbore failure. In: *Proceedings World Geothermal Congress 2010, Bali, Indonesia*.
- Valley, B. & Evans, K., Dec. 2009. Stress orientation to 5 km depth in the basement below Basel (Switzerland) from borehole failure analysis. *Swiss Journal of Geosciences* 102 (3), 467–480.
- Wood, A. T. A. & Chan, G. 1994. Simulation of stationary gaussian processes in  $[0, 1]$  d. *Journal of Computational and Graphical Statistics* 3 (4), 409–432.